

UNIVERSITAT DE BARCELONA
FACULTAT DE QUÍMICA
DEPARTAMENT DE QUÍMICA FÍSICA

Programa de Doctorat de Tecnologia de Materials

Bienni 2004-2006

**Electrochemical preparation of Co-Ag
nanostructured materials for GMR
applications**

Memòria que presenta JOSÉ MANUEL GARCÍA TORRES per optar al
títol de Doctor per la Universitat de Barcelona

Directores de la tesi:

Dra. Elvira GÓMEZ VALENTÍN
Professora Titular de Química Física
Universitat de Barcelona

Dra. Elisa VALLÉS GIMÉNEZ
Professora Titular de Química Física
Universitat de Barcelona

CHAPTER 5

Co-Ag/Ag MULTILAYERS

5

Co-Ag/Ag MULTILAYERS

Magnetic/non-magnetic multilayered films were a second kind of nanostructure of interest. In this chapter, some previous considerations about the electrodeposition process of magnetic multilayers are given in section 5.1. After that, a systematic study of the preparation of electrodeposited Co-Ag/Ag multilayers together with a detailed analysis of the structure and magnetotransport properties are shown in section 5.2.

5.1. Some considerations on multilayer electrodeposition

Different prerequisites for the achievement of the ferromagnetic/non-magnetic (FM/NM) layer structure with GMR must be considered. On one hand, the non-ferromagnetic behaviour of the non-magnetic layer, that is this layer must be void of any ferromagnetic impurity in order to exclude any undesirable electron scattering in this layer. As for the Co-Ag pair the deposition mode is normal, silver metal can be deposited without the incorporation of cobalt provided that silver deposition conditions are appropriate. On the other hand, the strongest ferromagnetic character of the magnetic layer is required since the non-magnetic metal incorporation during the magnetic metal deposition, which can not be avoided, is detrimental to the magnetic properties of the ferromagnetic layers.

In this sense, cobalt concentration in the electrolyte must be relatively high and also higher than that of silver in order to decrease silver incorporation during cobalt deposition to such a level that it does not impact the magnetic properties significantly. However, although silver concentration must be low, concentrations of the order of a few mmols dm⁻³ are required as lower concentrations would lead to some practical limitations during the multilayer electrodeposition

The electrodeposition of the magnetic multilayers is performed by alternatively switching the applied signal between two distinct values corresponding to the non-magnetic and magnetic metal deposition. Although different combinations can be made (see experimental section), the mixed galvanostatic/potentiostatic mode for Co/Ag deposition was selected.

5.1.1. Deposition conditions of the non-magnetic layer

In the current-controlled deposition mode (G mode), the optimum current that can be applied to electrodeposit the non-magnetic layer corresponds to the maximum current supplied by the electrolyte non-magnetic ions concentration, that is the diffusion current ($j_{\text{diffusion}}$), as currents out of this optimum value lead to undesired problems (Figure 5.1). Currents more negative than $j_{\text{diffusion}}$ would lead to the contamination of the non-magnetic layer with the magnetic metal. On the other hand, when the applied current density does not exceed the diffusion current the concentration of the non-magnetic element ions will not be zero close to the working electrode. The non-discharged ions can react with the less noble metal previously deposited via an exchange reaction, which can be written for the Co-Ag system as:



This exchange reaction implies that the real silver layer thickness will be certainly higher than that calculated from the Faraday's law; whereas the cobalt layer thickness will be significantly smaller.

The accurate determination of the diffusion current is a difficult task as minor changes in the electrodeposition conditions, i.e. ion concentration, temperature, pH or hydrodynamic conditions, can lead to a modification of it. Because of small changes in the diffusion current can lead to the undesired effects, the deposition of the non-magnetic metal is difficult to control by the galvanostatic mode.

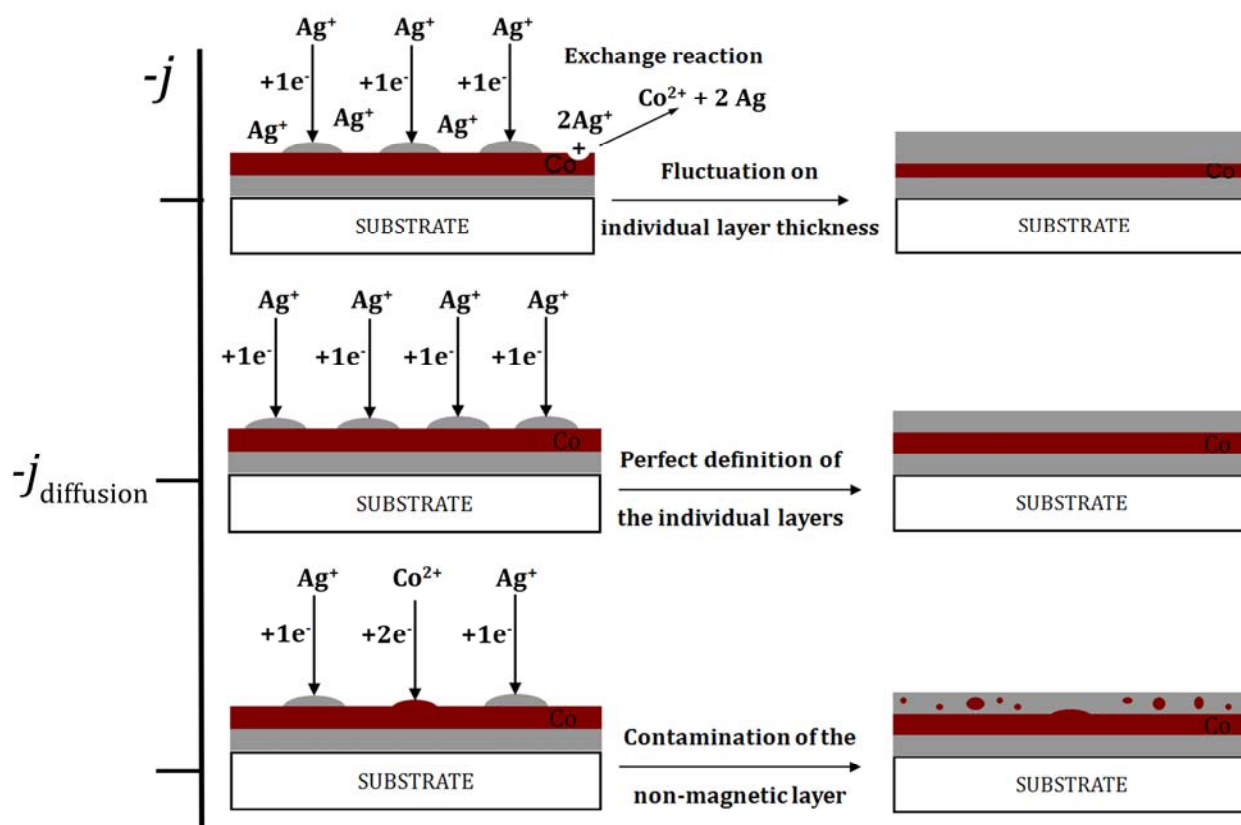


Figure 5.1. Problems during deposition of the non-magnetic layer by current control. On one hand, current density values more positive than $j_{\text{diffusion}}$ lead to the exchange reaction and therefore, a fluctuation on the magnetic and non-magnetic layer thickness. On the other hand, values more negative lead to the contamination of the non-magnetic layer with magnetic element. The optimum current value to prepare the non-magnetic layers corresponds to $j_{\text{diffusion}}$.

When the non-magnetic layer is deposited by potential control, the current will set to the diffusion current in the appropriate potential interval, so the exchange reaction is avoided by potentiostatic mode. However, silver deposition potential must be negative enough to prevent the dissolution of the previously deposited ferromagnetic layer but not too negative to allow cobalt codeposition. In any case, the potentiostatic mode is the preferred method as there is an electrodeposition condition range (a potential range) in which these phenomena can be avoided, unlike the galvanostatic mode in which the control of the electrodeposition conditions is difficult if not impossible. Although in the potentiostatic mode there is a potential interval to perform the electrodeposition, there is an optimum potential for the deposition of Ag of the non-magnetic layer. The optimization process for establishing this optimum potential will be discussed in section 5.2.

5.1.2. Deposition conditions of the magnetic layer

The deposition mode of the magnetic layer is not as critical as in the case of the non-magnetic layer. Although both deposition modes lead to well-defined magnetic layers, the galvanostatic mode is selected because a better control of the ferromagnetic layer composition is achieved than by potentiostatic deposition.

5.2. Electrodeposition and properties of Co-Ag/Ag multilayers

In view of the last section and the experienced gained in the *Electrodeposited nanostructures* group where this part of the thesis was carried out, it was decided to apply the potentiostatic mode for silver deposition and the current-control mode for cobalt deposition, the so called G/P mode, to grow the Co-Ag/Ag multilayers. The electrolytic bath employed to prepare the multilayers was the simplest bath as possible, containing only the metal salts and the supporting electrolyte. The reason was the deleterious effect of third species in the magnetoresistance. In order to obtain well-defined multilayered structures, the optimization of the electrodeposition conditions for both metals was carried out. The optimization of the magnetic layer consisted of looking for the electrodeposition conditions leading to layers with the lowest silver content. To achieve this objective, too low or too high currents must be avoided in order to make silver deposition and hydrogen evolution difficult, respectively. On the other hand, the optimum potential value for the non-magnetic layer deposition was that potential in which neither cobalt dissolution nor cobalt deposition took place along with silver deposition. In this sense, the examination of the current-time transients recorded by applying different potentials for silver deposition in the diffusion regime was fundamental.

Once the electrochemical parameters to grow the multilayers were established, it was proceed to prepare Co-Ag/Ag multilayers. Different parameters such as individual layer thickness or total thickness were modified in order to study their impact on the structure but mainly on the magnetotransport properties. Silver layer thickness was controlled by making flow the desired charge which was monitored by a computer-controlled data acquisition system. Meanwhile, pulse length was the parameter adjusted to control cobalt layer thickness. Thus, the applied signal was switched when the deposition charge for the silver layer or the deposition time for cobalt layer reached the set values.

Firstly, the magnetic and non-magnetic individual layer thicknesses were optimized. The layer thickness of both metals clearly modified the magnetotransport properties. GMR initially increased with silver layer thickness until reaching 6 nm thick layers, and then it dropped off for higher layer thicknesses. The same trend was observed for the GMR dependence on the cobalt thickness. The highest GMR value measured was for 3 nm thick cobalt layers. Further increase in the cobalt thickness gives rise to the appearance of a clear AMR contribution superimposed to the GMR. Thus, the highest GMR value measured (around 0.5%) was obtained for the samples with the layer structure Co-Ag (3nm)/Ag (6nm). On the other hand, no relevant influence of the total thickness on the GMR was observed.

At this moment and due to the low GMR values measured one raised oneself the question: Does the prepared films show a real multilayered structure? In view of the $MR(H)$ curves one could not assure it as two opposite effects were observed. On one hand, the non-saturating behaviour of the curves made think that the presence of superparamagnetic particles was important. On the other hand, the GMR peak position (H_p) value, which was significantly higher than that measured for d.c. plated cobalt-rich deposits, and the observed variation with the thickness of both the Co-rich layer and the non-magnetic layer, made think that an appropriate separation of the cobalt layers existed.

Further experiments shed light on this question. The decomposition of the $MR(H)$ curves into their superparamagnetic and ferromagnetic contributions and the structural characterization corroborated the no perfect multilayered structure of the prepared films. The small ferromagnetic contribution (which amounted up to 50 % at the very best) and the lack of satellite reflections⁽¹⁾ (Figure 5.2) revealed that magnetic layers were probably broken into SPM and FM regions, indicating the granular-type multilayered structure of the films prepared (Figure 5.3).

(1) A special feature of XRD is that, for multilayers of sufficiently good quality, so-called superlattice reflections [116] can appear in the XRD pattern which arise due to the periodic repetition of a bilayer unit in the XRD pattern.

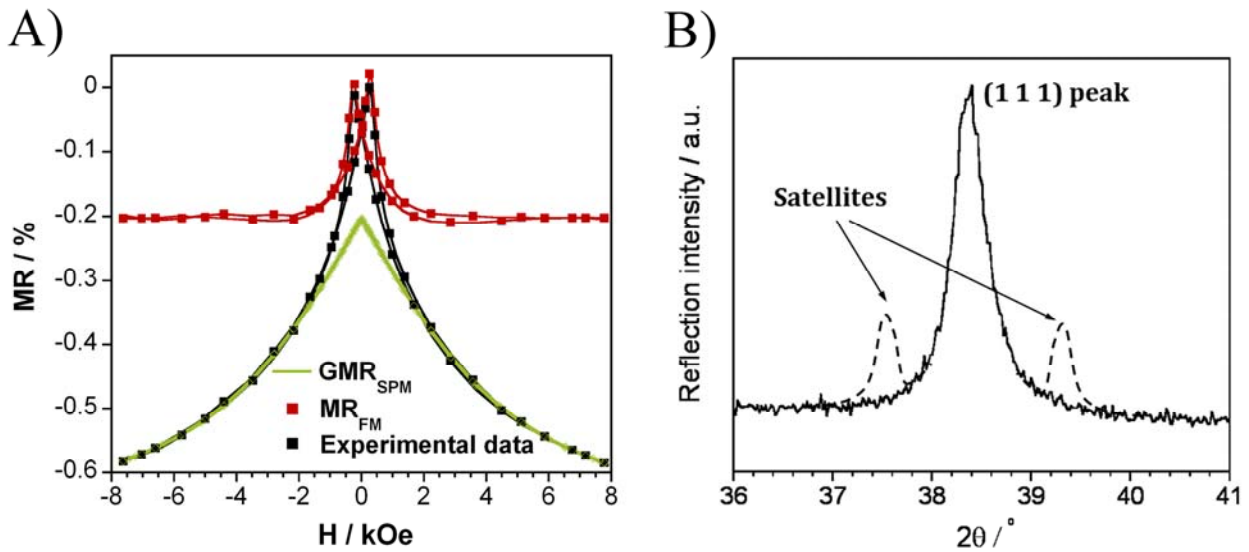


Figure 5.2. A) Decomposed $MR(H)$ curve showing the ferromagnetic (MR_{FM}) and superparamagnetic (GMR_{SPM}) contributions. B) Expected satellite reflections close to the diffraction peaks in well-defined multilayered structure.

Temperature was also observed to influence the magnetotransport properties of the films. GMR values increased up to 2 % as temperature decreased down to 20 K. However, the SPM contribution to the total MR scarcely changed with temperature. This is not usual as the ferromagnetic contribution is expected to be higher at lower temperatures because of more and more particles are blocked (became ferromagnetic) as temperature decreases. The dipolar interaction among the superparamagnetic regions explains this behaviour.

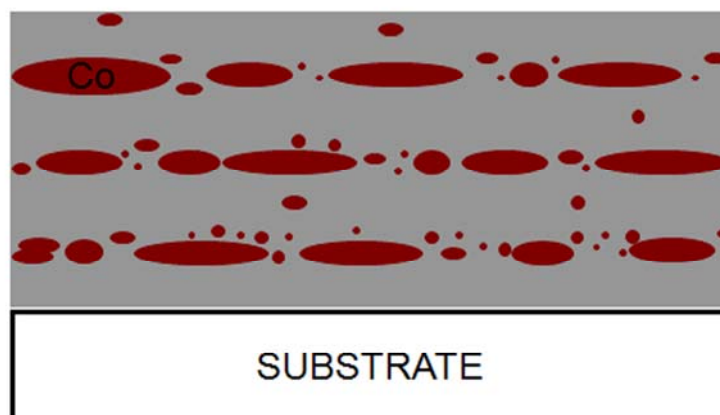


Figure 5.3. Scheme showing the granular-type multilayered structure expected in these samples.

GROUP OF ARTICLES INCLUDED IN SECTION 5.2.

Page 207: Preparation and giant magnetoresistance of electrodeposited Co-Ag/Ag multilayers

J. Garcia-Torres, L. Péter, A. Révész, L. Pogány and I. Bakonyi, Thin Solid Films 517 (2009) 6081

***Preparation and giant magnetoresistance
of electrodeposited Co-Ag/Ag multilayers***



Preparation and giant magnetoresistance of electrodeposited Co–Ag/Ag multilayers

J. García-Torres^{a,1}, L. Péter^{a,*}, Á. Révész^b, L. Pogány^a, I. Bakonyi^a

^a Research Institute for Solid State Physics and Optics, Hungarian Academy of Sciences, P.O. Box 49, H-1525 Budapest, Hungary

^b Department of Materials Physics, Eötvös University, P.O. Box 32, H-1518 Budapest, Hungary

ARTICLE INFO

Article history:

Received 19 February 2009

Received in revised form 4 May 2009

Accepted 5 May 2009

Available online 12 May 2009

Keywords:

Multilayer

Cobalt

Silver

Electrodeposition

Giant magnetoresistance (GMR)

ABSTRACT

Electrodeposition of Co–Ag/Ag multilayers along with their giant magnetoresistance (GMR) was investigated. The electrodeposition process was optimized for both minimizing the dissolution of the Co layer and achieving a high magnetoresistance. Structural analysis of Co–Ag/Ag deposits revealed that silver has an fcc structure, whereas cobalt crystallizes in the hcp structure. No solid solution of Co and Ag was detected. The X-ray diffraction study did not show any satellite reflection. A GMR of the order of 0.5% and 2% could be observed at room temperature and at 20 K, respectively, with both superparamagnetic and ferromagnetic GMR contributions throughout the temperature range studied.

© 2009 Elsevier B.V. All rights reserved.

1. Introduction

The phenomenon called giant magnetoresistance (GMR) was discovered some 20 years ago during the study of Fe/Cr multilayers [1,2]. The persistent interest in magnetic/non-magnetic multilayers is due to their application in data storage devices with magnetic recording. The discovery of the phenomenon was soon followed by the preparation of electrodeposited (ED) multilayers with GMR [3]. Electrodeposition is usually considered as a promising technique not only because of its simplicity compared with physical deposition techniques but also because it can produce high-quality multilayers [4], many of which exhibiting fairly large GMR values [5–7]. In the past 15 years, many types of (Ni, Co, Fe)/Cu multilayers were produced by means of electrodeposition, while the application of other non-magnetic (NM) metals in ED multilayers has remained rather scarce.

The present study is related to the preparation of Co–Ag/Ag multilayers. The reason for selecting this system is that the formation of sharp interfaces between the Ag and the Co-rich zones is expected due to the immiscibility of the constituents under equilibrium conditions.

In some previous studies [8–12], it has already been attempted to fabricate Co–Ag/Ag multilayers by electrodeposition. Valizadeh et al. [8] used a bath based on cobalt chloride or cobalt sulfate and silver cyanide. They prepared Co–Ag(5 nm)/Ag(5 nm) multilayers by galvanostatic deposition, with the magnetic layers containing a few percent of Ag only. Cross-sectional transmission electron micrographs

revealed a clear multilayered structure with fine grains, whereas X-ray diffraction (XRD) patterns indicated the presence of fcc–Ag and fcc–Co or hcp–Co layers without any multilayer satellite reflection. The broad XRD lines were also indicative of a fine-grained structure. No magnetic and magnetotransport data were reported.

The group of Ueda et al. [9,10] used a sulfate-based bath with sodium citrate addition to prepare magnetic/non-magnetic multilayers in the Co–Ag system by electrodeposition with current control. The composition of the layers was reported to be Co₇₀Ag₃₀/Co₈Ag₉₂. No structural characterization was given. Magnetization and magnetoresistance were found to depend on the thickness of both the Co-rich and the Ag-rich layers. The GMR at room temperature in a magnetic field of 1680 kA/m increased from about 5 to 9% when the thickness of the Co-rich layer changed from 0.4 nm to 1.6 nm. The GMR was also studied as a function of the Ag-rich layer thickness in the 0.3 nm to 1.8 nm range, and a maximum of about 9% was found at $d_{\text{Ag}} = 1.2$ nm. This GMR maximum increased to 13% at 5 K [10].

Later, Ueda et al. [11] reported current-controlled electrodeposition of Co–Ag/Ag multilayers from a bath containing CoSO₄ and AgI. Whereas the magnetic layer was found to be of the same composition as in their previous works [9,10], the composition of the NM layers was not specified at all and structural data were not reported either. For these multilayers, the GMR exhibited a maximum of about 6 to 7% as a function of the layer thicknesses. The GMR maximum was achieved between 0.5 nm and 1.5 nm for each layer, the exact position depending slightly on the thickness of the other layer.

Finally, the work of Fedosyuk et al. [12] has to be mentioned. They reported electrodeposition of Co–Ag/Ag multilayers from a bath containing CoSO₄ and AgNO₃ by means of current control. The magnetic layer contained some 10–15 at.% Ag. XRD measurements

* Corresponding author. Tel.: +36 1 392 2222x3614; fax: +36 1 392 2215.

E-mail address: lpeter@szfki.hu (L. Péter).

¹ On leave from the Laboratory of Electrodeposition and Corrosion, University of Barcelona, Spain.

revealed the presence fcc–Ag and fcc–Co phases in the as-deposited state for magnetic layer thicknesses smaller than about 100 nm. A GMR of about 0.7% was observed at room temperature in a magnetic field of about 640 kA/m for a multilayer with unspecified layer thicknesses. The magnetoresistance curve exhibited a single peak at zero magnetic field, which changed to a symmetrically split double-peaked curve after annealing at 400 °C for 30 min. At the same time, the maximum GMR reduced to about the half of the value measured in the as-deposited state. Although no XRD patterns were presented, these authors claimed that the heat-treated sample exhibited satellite diffraction peaks around the fcc–Co reflections. The repeat distance calculated from the satellite peak positions was found to be in good agreement with the nominal bilayer thickness.

As the above summary reveals, the preparation of ED multilayers in the Co–Ag system was carried out in all previous works [8–12] by means of current control only and the structural characterization of these multilayers was either missing or not properly documented. As it is well-known [7], an exchange reaction takes place inevitably during the galvanostatic deposition of the more noble metal, strongly influencing the actual layer thicknesses. This exchange reaction can be formulated in general as $l MN^{m+} + m LN = l MN + m LN^{l+}$, MN and LN being the more noble and the less noble metal, respectively. Hence, the thickness of the less noble magnetic metal layer will be smaller and the thickness of the more noble NM layer will be larger than the corresponding nominal values. The magnetic layer dissolution during the deposition pulse of the NM layer promotes the formation of superparamagnetic (SPM) regions [13,14]. This leads to a high saturation field of the magnetoresistance in electrodeposited multilayers as one can also see for the Co–Ag system where the field-dependence of the magnetoresistance was reported at all [9,10,12].

In view of the rather incomplete character of the above mentioned reports, we decided to perform a comprehensive study of the preparation of electrodeposited Co–Ag/Ag multilayers. Not only the electrochemical optimization process with the help of the selected electrolyte is reported, but also a characterization of the electrodeposited films from the viewpoints of structural and magnetotransport properties is given in detail. Special emphasis was put on utilizing the results of recent developments in optimizing the electrochemical conditions for multilayer preparation by electrodeposition [7,15] and in analyzing the GMR data by separating the ferromagnetic (FM) and SPM contributions [14].

2. Experimental details

2.1. Sample preparation

Electrodeposition was performed in a tubular cell of 8 mm × 20 mm nominal cross section with an upward facing cathode at the bottom of the cell [13,16]. A saturated calomel electrode (SCE) was used as reference electrode, and potentials are given accordingly throughout this paper. The counter electrode was a platinum wire. For potentiodynamic experiments and for recording potentiostatic current transients, Ni foils were used as working electrode. Nickel was inert (and probably passive) in the solutions used and, hence, it had a negligible contribution to the current recorded. The multilayers prepared for magnetotransport measurements and structural studies were deposited onto Si(100)/Cr (5 nm)/Cu(20 nm) substrates. The Cr adhesive layer and the Cu seed layer were prepared by evaporation on the Si wafer. In each case, electrodeposition was performed at room temperature with no stirring.

Solutions containing $\text{Co}(\text{ClO}_4)_2$, AgClO_4 and NaClO_4 were prepared with analytical grade chemicals and ultrapure water (ELGA Purelab). The pH of the electrolytes was between 2.0 and 2.5, depending on the concentration of the metal salts. Multilayers were prepared by using the G/P mode [7,13] developed in our laboratory. In this method, a galvanostatic (G) and a potentiostatic (P) pulse is applied alternately for the deposition of the magnetic and the non-magnetic layers,

respectively. A computer-controlled EF 453 potentiostat/galvanostat (Electroflex, Hungary) was used for all types of electrochemical experiments. The Ag deposition potential was optimized according to the method described in Ref. [15], which ensured that neither Co dissolution nor Co deposition occurred during the Ag deposition pulse. The layer thicknesses were controlled via the pulse length in the G mode, while a real-time current integration was used to determine the charge passed through the cell in order to monitor the layer growth in the P mode. The number of bilayer repeats was varied in a manner as to maintain a nearly constant total multilayer thickness of about 800 nm, except for the cases when the influence of the total thickness on the magnetoresistance was studied.

2.2. Characterization of the deposits

A non-destructive chemical analysis of several multilayer deposits was performed by the electron probe microanalysis facility of a JEOL JSM 840 scanning electron microscope.

XRD was used to investigate the structure of the deposits. A Philips equipment with Cu K α radiation (wavelength: 0.15406 nm) was used to carry out XRD measurements on the multilayers on their substrates. The structure was also studied with high-resolution transmission electron microscopy (HRTEM) by using a Phillips CM30 equipment combined with electron diffraction. In order to perform the HRTEM study, the samples were polished mechanically and then thinned by means of Ar⁺ ion bombardment to achieve the appropriate thickness which allows electrons to pass through the sample (around 100 nm). After that, the samples were mounted on a copper holder. The acceleration voltage during the HRTEM study was 200 kV.

Magnetoresistance data were measured in the field-in-plane/current-in-plane geometry on 1 to 2 mm wide strips with the four-point contact method, using magnetic fields up to 640 kA/m. Both the longitudinal (LMR, field parallel to current) and the transverse (TMR, field perpendicular to current) magnetoresistance components were measured. The following formula was used for calculating the magnetoresistance ratio: $\Delta R/R_0 = (R_H - R_0)/R_0$ where R_H is the resistance in a magnetic field H and R_0 is the resistance value of the magnetoresistance peak around zero field. The shunt effect of the substrate was not corrected. Magnetoresistance data at low temperature were measured in a closed-cycle He cryostat (made by Leybold).

3. Results

3.1. Optimization of the deposition conditions

Recently, a perchlorate-based electrolyte was developed and characterized electrochemically [17,18] for the electrodeposition of Co–Ag alloys. In the present work, we started the electrochemical preparation of multilayers in the Co–Ag system on the basis of this bath composition. However, in view of previous experience with solutions containing so-called brighteners and other additives such as, e.g., stress-reducing agents and surfactants, which were found to be deleterious for the GMR of ED multilayers [19,20], we have here omitted all ingredients from the original Co–Ag bath [17,18] except for the perchlorate components.

For obtaining deposits with well-defined magnetic to non-magnetic layer thickness ratios, it was an important task to optimize the electrodeposition process. For this purpose, the concentration of the metal salts and the electrochemical parameters (current density, potential, deposition time) were adjusted so as to obtain deposits with the highest achievable GMR.

3.1.1. Optimization of magnetic layer deposition: characterization of d.c.-plated Co-rich deposits

The desired ferromagnetic behaviour of the magnetic metal (magnetic layer) is essential to prepare multilayers with GMR. According to the general experience, a sufficiently large anisotropic

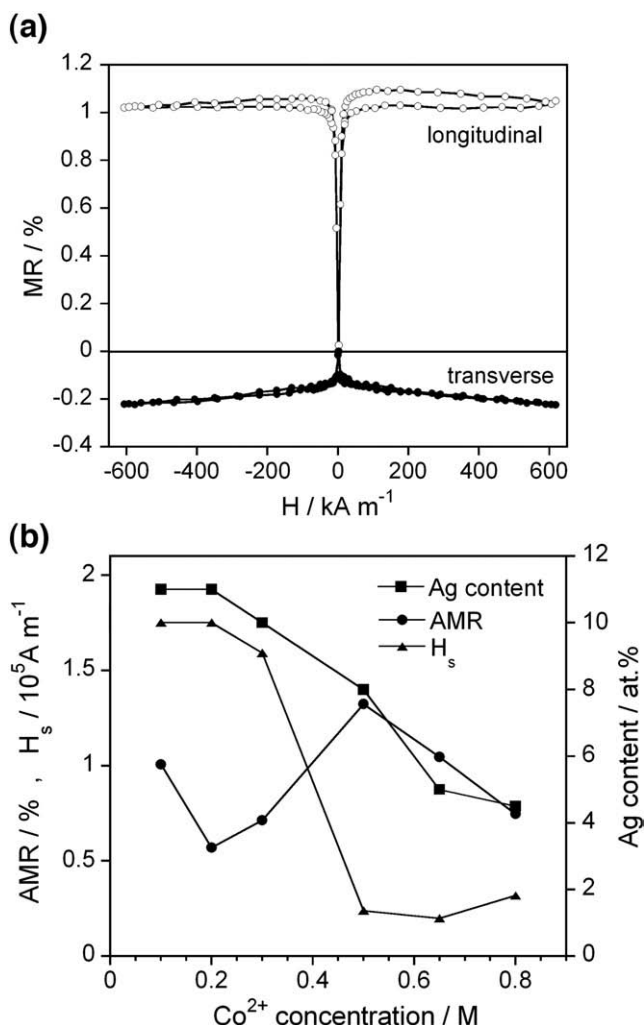


Fig. 1. (a) Longitudinal (LMR) and transverse (TMR) components of the magnetoresistance for a d.c.-plated Co-rich deposit prepared from a bath containing 0.5 M CoSO_4 . (b) AMR, magnetoresistance saturation field H_s (left axis) and Ag concentration of the deposit (right axis) as a function of the Co ion concentration in the bath.

magnetoresistance (AMR) of the bulk ferromagnetic metal is crucial for obtaining multilayers with large GMR. With this rule of thumb in mind, an optimization process was carried out by looking for deposition conditions at which electrodeposited cobalt (or, actually, a Co-rich Co–Ag alloy) exhibited a ferromagnetic behaviour comparable to that of bulk Co (with saturation field $H_s \approx 80$ kA/m and $AMR \approx 1$ –2% [21]). For this purpose, a series of cobalt-rich deposits was prepared in which both the Co^{2+} ion concentration and the current density were varied in a manner that the ratio $j_{\text{Co}}/[\text{Co}^{2+}]$ (where j_{Co} is the Co deposition current density) was kept constant. The current density was smaller than the transport-limited current density of Co in all cases, but it was high enough to deposit silver at the limiting current even in the case of the smallest $[\text{Co}^{2+}]$ value. Without increasing the current density with $[\text{Co}^{2+}]$, the increase of the cobalt ion concentration would lead to a very little change only in the Co content of the deposit. The present method ensured that deposits with increasing Co:Ag ratios were obtained, and the onset of the appropriate ferromagnetic properties could be observed without using an unduly large excess of the Co^{2+} source compound in the bath.

Fig. 1(a) shows the room-temperature magnetoresistance curves for a typical Co-rich deposit obtained by d.c.-plating. This deposit exhibited a ferromagnetic behaviour similar to that of bulk Co: positive LMR and negative TMR components are obtained with $AMR = LMR - TMR$ value amounting to some 1%, and saturation was

achieved in magnetic fields of about 80 kA/m. Beyond this field, the magnetoresistance curve had a linear section with slowly decreasing magnetoresistance, which is typical for all FM metals due to the so-called paraprocess [22].

The magnetoresistance curves measured for several d.c.-plated deposits obtained for different Co^{2+} ion concentrations in the bath were qualitatively similar to that shown in Fig. 1(a). The chemical analysis of d.c.-plated deposits revealed a decrease in the silver content of the deposits with increasing cobalt concentration in the bath (see Fig. 1(b)). The AMR magnitude and magnetoresistance saturation field (H_s) are also displayed as a function of the Co^{2+} ion concentration in the bath in Fig. 1(b). Whereas the AMR magnitude is around 1% in each case, the saturation field shows a systematic dependence on the Co^{2+} ion concentration. At a Co^{2+} ion concentration of 0.5 M, the AMR is fairly high and the deposit is magnetically sufficiently soft, with a saturation field lower than 30 kA/m. Therefore, this Co^{2+} ion concentration was chosen for preparing multilayers since this bath with the corresponding current density ($j_{\text{Co}} = -35$ mA/cm²) can provide an appropriate magnetic layer as a multilayer constituent. Above 0.5 M cobalt ion concentration and at the corresponding high current densities, strong hydrogen evolution could be observed which decreased the current efficiency and, hence, hindered the formation of a continuous deposit with higher Co content. Another impact of the hydrogen evolution on the multilayer preparation was that the pH increased in the vicinity of the cathode and the Co deposited during the high-current pulse was oxidized in the next pulse, hence preventing the formation of an Ag layer.

3.1.2. Optimization of silver layer deposition

For the deposition of the silver layer, it must be considered that too positive silver reduction potentials could give rise to the dissolution of the less noble metal, while very negative potentials could imply the codeposition of both metals during silver layer formation. Both effects are counterproductive to reach a high GMR value. Therefore, the deposition conditions of Ag also need to be optimized.

The first step of the optimization of Ag deposition was the establishment of the onset potential of Ag deposition, the potential range of the diffusion-limited Ag deposition, the onset potential of other reduction processes and the dissolution potential of both metals. This was performed by recording conventional potentiodynamic curves shown in Fig. 2 for various cathodic limits.

At low cathodic limits (–600 mV), only one reduction process is observed with the onset potential of 510 mV. The corresponding process is the reduction of the Ag^+ ions and the formation of a silver deposit. The current density observed right after reaching the onset

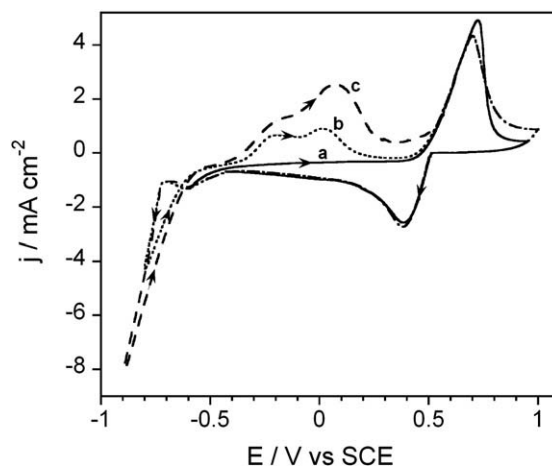


Fig. 2. Potentiodynamic curves recorded with various cathodic limits for an electrolyte containing 0.5 M $\text{Co}(\text{ClO}_4)_2$ + 0.01 M AgClO_4 + 0.1 M NaClO_4 . Cathodic limits: (a) –600 mV, (b) –800 mV, (c) –900 mV. Sweep rate: 50 mV s⁻¹.

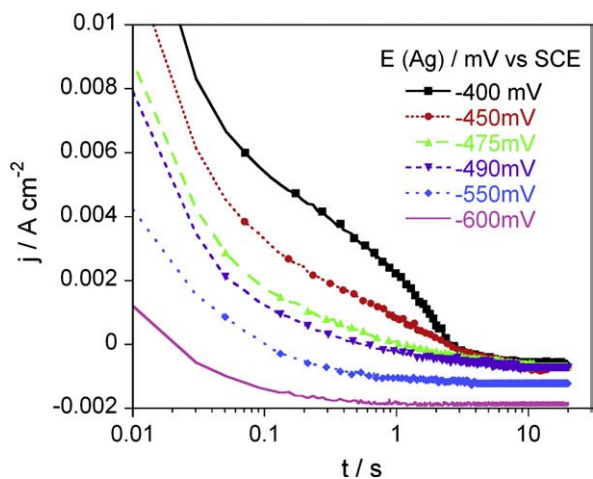


Fig. 3. Current transients recorded for the Ag deposition pulse during the deposition of Co-Ag multilayers in the G/P mode. Electrolyte: 0.5 M $\text{Co}(\text{ClO}_4)_2 + 0.01 \text{ M AgClO}_4 + 0.1 \text{ M NaClO}_4$. For other details, see the text.

potential went through a maximum, then decayed and approached to a constant current density, indicating that the reduction process became diffusion-limited. Although the cathodic current increased slightly at potentials more negative than -450 mV , the positive-going scan exhibited cathodic current only until the potential reached the value where the deposition of silver started. The shape of the anodic peak observed at potentials more positive than 510 mV corresponds to a stripping peak since it starts with an exponential increase followed by a very sharp decay as the dissolution of the deposit finished. The $\text{Ag}^+ + e = \text{Ag}$ process is reversible, as shown by the agreement of the onset potentials of the deposition and dissolution.

By performing scans with more negative limits, the current increase starting at -450 mV was observed again, giving rise to a peak centered at -600 mV . The amplitude of this peak was small compared to the Ag deposition peak, and it is thought to be related to the H^+ reduction process. The deposition of cobalt started at -715 mV . It was clear from the shape of the voltammograms that the Co deposition process was significantly influenced by the nucleation barrier of Co on Ag. The diagnostic criterion of the high nucleation barrier is that the positive-going section of the potentiodynamic curve exhibited larger cathodic currents than the previous negative-going sweep and the current related to the Co deposition process prevailed till a considerably more positive potential than the onset potential of Co deposition. The current density during the positive-going sweep returned to the value of the diffusion-limited Ag deposition at -550 mV only.

The dissolution of Co takes place in the -460 mV to $+300 \text{ mV}$ potential interval, and two peaks centered at -200 mV and 70 mV appear in the positive-going scan. Similar pairs of anodic peaks are observed in the anodic-going sweeps for Co-Cu [15,23] and Co-Ag baths [24–26]. The origin of the peak with the more negative potential is uncertain. This peak is often attributed to the desorption of hydrogen even if no hydrogen adsorption peak is observed, but it is also possible that it corresponds to the dissolution of Co. The latter explanation may originate from the fact that the deposition of silver is not stopped while Co was codeposited, and the various Co-Ag alloys may have different dissolution potentials. This is supported by the finding that a slight modification of the starting potential of the most negative peak towards negative values is also detected when increasing the cathodic limit. It can also be seen that the higher the cathodic limit, the higher the intensity of both peaks in the cobalt dissolution regime (see Curve c in Fig. 2).

Based on the latter observations, it was decided to study the silver deposition during the multilayer formation in the potential range of -400 mV to -600 mV by means of the analysis of potentiostatic

current transients. It was expected that the appropriate Ag deposition potential for avoiding both Co dissolution and Co codeposition lies in this potential range. The study of the current transients during the deposition of multilayers was performed the same way as described in our previous work [15].

In each pulse-plating experiment, the 30th cycle was analyzed in order to eliminate any possible substrate effect and also to achieve a steady-state pulse behaviour. The Co-rich magnetic layer was obtained at a fixed current density of -35 mA cm^{-2} and a fixed time of 0.254 s , and hence with a constant charge of -9 mC cm^{-2} . The nominal Co-rich layer thickness corresponding to this charge is 3 nm . The silver layer was deposited at a constant potential, varying it in the range of -400 mV to -600 mV as previously established. The Ag deposition charge was set to -2.8 mC cm^{-2} giving a nominal silver layer thickness of 2.7 nm by assuming 100% current efficiency.

Fig. 3 shows a few current transients recorded for the potentiostatic silver deposition pulse. As it can be observed in this figure, an initially positive current was recorded for all potentials studied. This positive contribution arises from two phenomena: first, the charge/discharge of the Helmholtz layer at the metal-solution interface and, second, the cobalt dissolution. The more negative the potential is, the shorter the transient period is and the smaller the anodic current is at the beginning of the pulse. Another remarkable feature of the curves is that at the most positive potentials the current becomes almost constant after a few seconds only, reaching the diffusion-limited Ag^+ reduction current after the total coverage of cobalt by the silver layer. As the Ag deposition potential is chosen more negative, the limiting current is reached within a shorter period of time due to the decrease of the rate of cobalt dissolution. However, at -550 mV and more negative potentials a larger limiting current density was observed as the H^+ reduction started. Codeposition of Co with Ag is also possible at potentials more negative than -500 mV , i.e., at potentials where Co deposition was observed in the anodic scans of the potentiodynamic curves (see Fig. 2).

In order to minimize both the dissolution and the deposition of cobalt during the silver layer formation, the potential of Ag deposition for preparing Co-Ag multilayers was selected to be -490 mV .

3.2. Structural characterization

For describing the structure of Co in ED Co-Ag samples, d.c.-plated Co-rich deposits were first analyzed by XRD. As it can be seen in Fig. 4, pure cobalt deposits exhibit a mixture of both fcc and hcp structures. When a small amount of silver (10 at.%) was present in the deposit, the XRD patterns revealed strong Ag peaks compared to the Co peaks. With the codeposition of Ag, the intensity of some Co peaks decreased (see peaks at $2\theta = 41.8^\circ, 47.5^\circ$ and 76°).

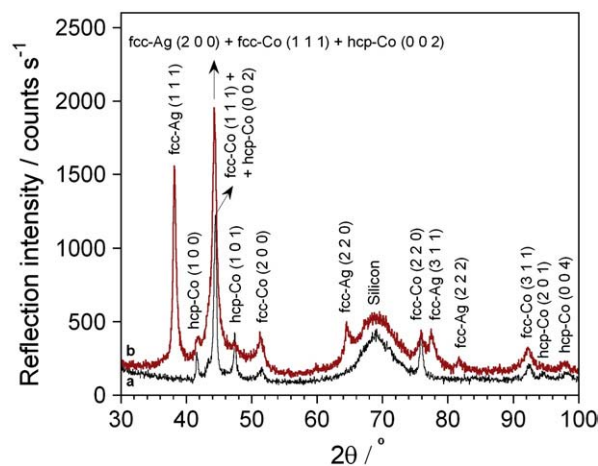


Fig. 4. XRD pattern of d.c.-plated Co-rich deposits without (a) and with 10 at.% Ag (b).

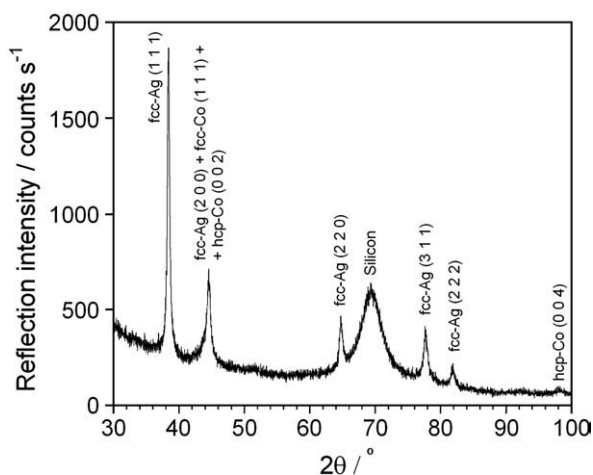


Fig. 5. XRD pattern of a Co-Ag(3 nm)/Ag(6 nm) multilayer. The sample was on its Si/Cr/Cu substrate.

Another important finding is the shift in some fcc-Co peaks when silver is incorporated in the deposit, indicating some solid solution formation. The calculated fcc-Co lattice parameter (0.3599 nm) from the XRD patterns is higher than the literature data (0.35441 nm), a fact that can be explained by the Ag incorporation in the fcc-Co lattice.

The structure of Co-Ag/Ag multilayers with different silver layer thicknesses (2 nm, 6 nm and 10 nm) was also analyzed by XRD. Fig. 5 shows the diffractogram of a typical Co-Ag/Ag multilayer on its Si/Cr (5 nm)/Cu(20 nm) substrate. Besides the diffraction peak due to the Si substrate, several peaks corresponding to the deposit were detected. Most of these peaks correspond to a polycrystalline fcc-Ag structure. Meanwhile, Co peaks were not observed or overlapped with silver peaks, making it difficult to establish the structure of the Co-rich magnetic layer within the multilayers. It is remarkable that no shift in the silver peak positions was detected when the diffractograms of multilayers with different Ag-layer thicknesses were compared. Moreover, the calculated silver lattice parameter (0.40830 nm) was in agreement with the literature data for pure Ag (0.40779 nm). Furthermore, no multilayer satellites were observed in any of the films studied, not even for the thickest silver layer, which is either the indication of a non-coherent growth of the subsequent layers or that of the undulated layer interfaces (or perhaps both). It is also possible that discontinuous layers were obtained since the immiscibility of Co and Ag is accompanied with a lattice mismatch of about 14%, introducing high interface energy between the Co and Ag layers.

HRTEM together with selected area electron diffraction (SAED) was used as this technique provides additional information about the crystal structure. Fig. 6 shows the SAED pattern of a Co-Ag/Ag multilayer sample and Table 1 gives the indices of the corresponding

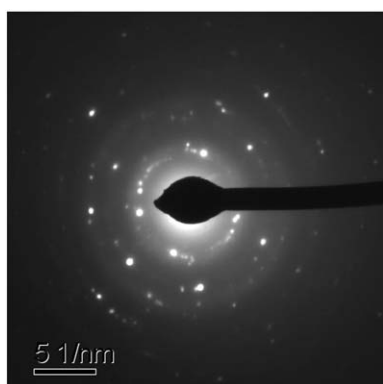


Fig. 6. SAED pattern of the same Co-Ag(3 nm)/Ag(6 nm) multilayer as in Fig. 5.

Table 1

Comparison of lattice plane distances measured in the SAED pattern of a Co-Ag/Ag multilayer and the tabulated JCPDS data.

Measured lattice plane distance (nm)	Lattice plane distance in fcc-Ag (nm)	Lattice plane distance in hcp-Co (nm)	Lattice plane distance in fcc-Co (nm)
0.2343	0.23587 (111)		
0.2164		0.21697 (100)	
	0.20427 (200)	0.20446 (002)	0.20461 (111)
0.1875		0.19166 (101)	
			0.17720 (200)
0.1492	0.14444 (220)	0.14880 (102)	
0.1275	0.12318 (311)	0.12527 (110)	0.12530 (220)
	0.11793 (222)	0.11542 (103)	

(The corresponding lattice plane index is given in parenthesis. The multilayer sample is the same as that in Figs. 5 and 6).

diffraction rings. The analysis of the patterns indicated the presence of fcc-Ag and hcp-Co. The SAED pattern also revealed that no fcc-Co phase was present as the most important reflections ((111) and (200)) were not detected.

3.3. Magnetoresistance of the multilayer samples

Fig. 7 shows typical room-temperature magnetoresistance curves obtained for the Co-Ag/Ag multilayer samples. A clear GMR behaviour was observed for all samples since both LMR and TMR are negative in the whole field range, LMR being always slightly smaller in magnitude than TMR. A splitting of the magnetoresistance curves occurred for all the samples studied. The saturation of the magnetoresistance curves could not be achieved up to the 640 kA/m field limit.

3.3.1. Impact of the deposition potential of the Ag layer on the magnetoresistance

The influence of the silver deposition potential on the GMR was investigated in a narrow potential range around the optimum Ag deposition potential of -490 mV as deduced from Fig. 3. Fig. 8 shows the variation of the total GMR with the applied potential. It can be seen that a sharp maximum value is reached at -490 mV. The data in Fig. 8 confirm the conclusion drawn from the current transient curves presented in Fig. 3. At potentials more positive than -490 mV, cobalt dissolution proceeds, which makes the cobalt layer fragmented. If the potential is more negative than the optimized one, cobalt deposition can take place during silver reduction, leading to a decrease in

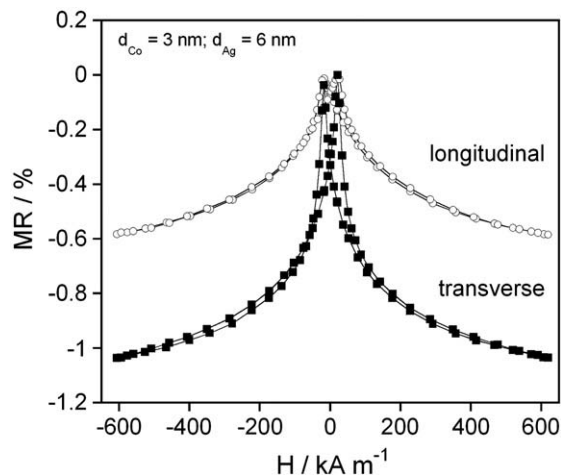


Fig. 7. Longitudinal and transverse MR curves of the electrodeposited Co-Ag(3 nm)/Ag(6 nm) multilayer.

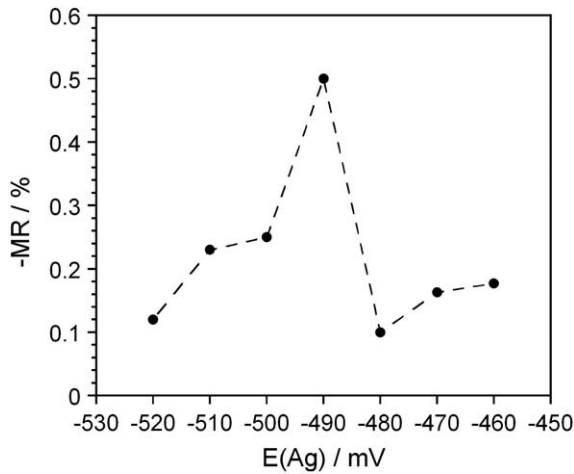


Fig. 8. Magnetoresistance of electrodeposited Co–Ag(3 nm)/Ag(6 nm) multilayers obtained at different silver deposition potentials. The MR was measured at $H = 640$ kA/m.

magnetoresistance due to the contamination of the NM layer with magnetic atoms.

3.3.2. Room-temperature magnetoresistance: Layer thickness dependence

First, the influence of the total film thickness on magnetoresistance was investigated. No variation in the magnitude of the GMR measured at the maximum available field was observed when the total multilayer thickness was varied from 200 nm to 800 nm. Therefore, the maximum total sample thickness (800 nm) was applied for studying the impact of the Co and Ag layer thicknesses.

The peak position (H_p) of the longitudinal magnetoresistance curves is displayed in Fig. 9 as a function of both the magnetic and non-magnetic layer thicknesses. As it is known from previous studies on electrodeposited Co–Cu/Cu [27] and Co–Ni–Cu/Cu [28] multilayers, GMR peak position correlates well with the coercive field (H_c); therefore, Fig. 9 shows approximately the dependence of the coercive field on the layer thicknesses. It is noted that the coercive field of the d.c.-plated Co-rich deposits, on the basis of the AMR curves in Fig. 1(a), is well below 10 kA/m whereas the coercive field of the electrodeposited Co–Ag/Ag multilayers in Fig. 9 all exhibit values above 16 kA/m. This is due to the fact that in magnetic thin films the coercive field can be significantly higher than in the bulk form of the same magnetic material [29] and strongly increases with decreasing magnetic layer thickness.

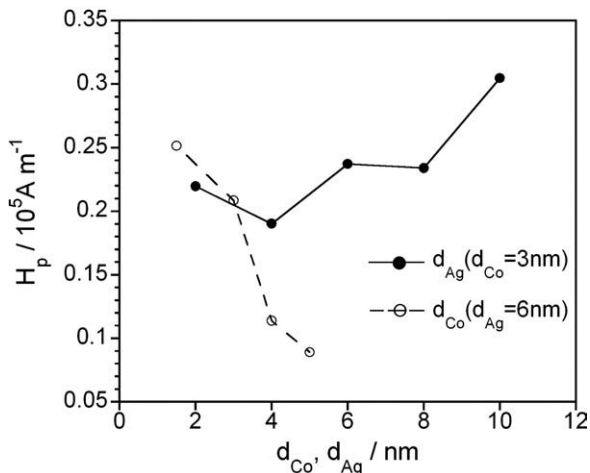


Fig. 9. Magnetoresistance peak position H_p of electrodeposited Co–Ag/Ag multilayers as a function of the thickness of the magnetic and the non-magnetic layer.

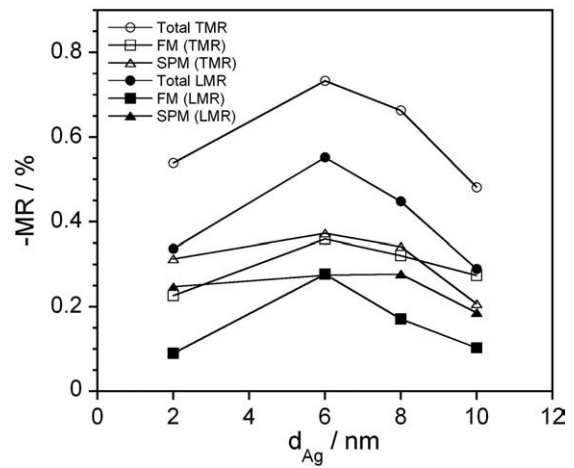


Fig. 10. Results of the decomposition of the $MR(H)$ curves into SPM and FM contributions as a function of the silver layer thickness.

The data shown in Fig. 9 are in good agreement with former results on the magnetic layer thickness dependence in electrodeposited Co–Cu/Cu multilayers [27]. This indicates that the Co-rich magnetic layers in the present Co–Ag/Ag multilayers with $d_{Ag} > 2$ nm can be considered as being well separated from each other since the presence of pinholes in the Ag-layers would result in a bulk-like behaviour with much lower coercive forces than observed.

The Ag-layer thickness dependence indicates a slight variation of the H_p values between 19 kA/m and 24 kA/m in the range of $d_{Ag} = 2$ nm to 8 nm. At $d_{Ag} = 10$ nm, the H_p value reaches almost 32 kA/m. These data suggest that there is an appropriate separation of the magnetic layers in the whole range of Ag layer thicknesses. The threshold Ag layer thickness where the Co layer separation is already imperfect and hence an AMR behaviour can be obtained was not investigated, although the occurrence of AMR is expected below a certain spacer layer thickness, similarly to electrodeposited Co–Cu/Cu multilayers [27].

A common feature of the magnetoresistance curves of all electrodeposited Co–Ag/Ag multilayers in this work is that the magnetoresistance does not show saturation up to high magnetic fields. This observation is common for many electrodeposited multilayer systems [3,5–7,27] and also for practically all former reports on ED Co–Ag/Ag multilayers [9–12]. For this reason, the procedure suggested in Ref. [14] was applied to separate the magnetoresistance into FM and SPM contributions. Briefly, one can describe the $MR(H)$ data for magnetic fields $H > H_s$ in the form [14]

$$MR(H) = MR_{FM} + GMR_{SPM}L(x), \quad (1)$$

where $MR_{FM} = AMR + GMR_{FM}$ is a constant term, H_s is the saturation field of the FM contribution and $L(x)$ is the Langevin function where $x = \mu H/kT$ with μ constituting the average magnetic moment of a SPM region.

In order to know the proportion of the GMR_{SPM} and GMR_{FM} contributions to the total magnetoresistance measured, the appropriate numerical analysis of the field dependence of the magnetoresistance was made on the basis of Eq. (1). The measured $MR(H)$ data are fitted with the Langevin function for magnetic fields beyond the FM saturation ($H_s \approx 160$ kA/m) for both the LMR and TMR components and this provides the $GMR_{SPM}(H)$ contribution. When subtracting this contribution from the experimental data, we are left with the $MR_{FM}(H)$ contribution.

It turned out from the above described decomposition of the $MR(H)$ curves that the SPM contribution is usually somewhat larger than the FM one (see Fig. 10). Independently of the individual cobalt or silver

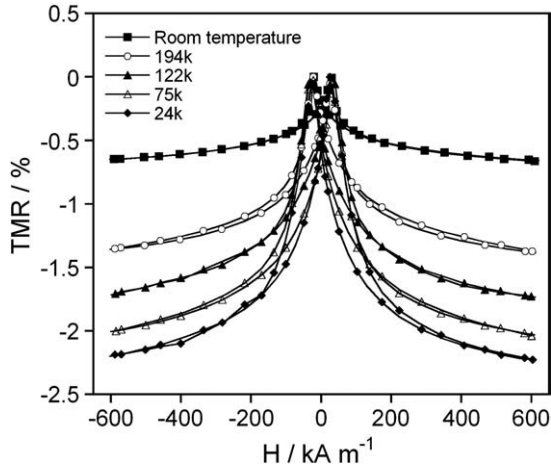


Fig. 11. Temperature dependence of the transverse magnetoresistance for a Co–Ag (3 nm)/Ag(6 nm) multilayer.

layer thickness, one can deduce the lack of continuous magnetic layers because of the high GMR_{SPM} contribution as compared to the GMR_{FM} contribution. These findings reveal that “FM region → NM region → SPM region” (or in the opposite direction) is the main electron-travel pathway for spin-dependent scattering events [14].

3.3.3. Temperature dependence of the magnetoresistance

The highest magnetoresistance value was obtained for the samples with the layer structure Co–Ag(3 nm)/Ag(6 nm) and with a total film thickness of 800 nm. The temperature dependence of the magnetoresistance was studied for this sample. Both longitudinal and transverse components were measured at different temperatures down to 24 K. The TMR results are displayed in Fig. 11 (it is noted that the LMR curves exhibited a similar character).

As it can be observed in Fig. 11, the lower the temperature, the higher the GMR recorded. However, regardless of the low temperature, none of the magnetoresistance curves (neither LMR nor TMR) showed saturation up to the highest magnetic field applied, indicating again the large contribution of the SPM entities to the total magnetoresistance at all temperatures studied. In order to analyze quantitatively the contribution of both FM and SPM regions, the decomposition process of the GMR curves was also performed with the data recorded at each temperature. The decomposition results are shown in Fig. 12(a) for both LMR and TMR. One can observe that both FM and SPM contributions increase roughly linearly with decreasing temperature in almost the same proportion; in other words, the relative weight of the SPM contribution to GMR scarcely changes with temperature. The conclusion to be drawn from this result is that the relative importance of the various spin-dependent scattering events is independent of temperature. Similar results were obtained for ED Co–Cu/Cu ML samples [30].

The decomposition procedure revealed that the fractional SPM contribution to the total magnetoresistance is practically the same, regardless of in which geometry the measurement was performed; i.e., whether the LMR or the TMR curves are analyzed. This observation is in a good agreement with the origin of AMR since it is related to consecutive spin-dependent scattering events within the same FM region.

Fig. 12(b) shows the temperature dependence of the average moment μ of the SPM regions obtained from the analysis of the magnetoresistance curves. A decrease in the value of μ with temperature can be seen, a finding which could be explained by the blocking of smaller and smaller clusters with decreasing temperature. However, the SPM character of the magnetoresistance curves was retained at low temperatures, suggesting the idea that by far not all SPM regions could be blocked even at the lowest temperatures applied.

Since the last two statements are contradictory, the data were analyzed according to the model of interacting SPM regions applied for Co–Cu/Cu multilayers [30] and Co–Cu granular alloys [31]. According to the theorem of interacting SPM particles [31], the magnetic dipolar interactions between the SPM regions (and, to a lesser extent, between the SPM and FM entities) can be effective if they are sufficiently close to each other. This interaction explains the constancy of the fractional SPM contribution to the total GMR when the temperature is varied and, hence, the much lower rate of saturation of magnetoresistance than in the absence of this interaction. The model involving the magnetic interaction could also explain the decrease in the apparent SPM cluster size with temperature [30,31]. The framework established for studying the interacting behaviour of SPM regions [30,31] requires the reformulation of the expression of magnetoresistance:

$$MR(H) = MR_{FM} + GMR_{SPM}L\left(\frac{\mu'H}{k(T + T^*)}\right) = MR_{FM} + GMR_{SPM}L\left(\frac{H}{k\lambda}\right) \tag{2}$$

where the meaning and the value of MR_{FM} and GMR_{SPM} are identical to those used in Eq. (1), μ' is the actual SPM magnetic moment and the term T^* is introduced to characterize the SPM dipolar interaction. The parameter $\lambda = T^*/\mu' + T/\mu'$ is defined to simplify the fitting procedure.

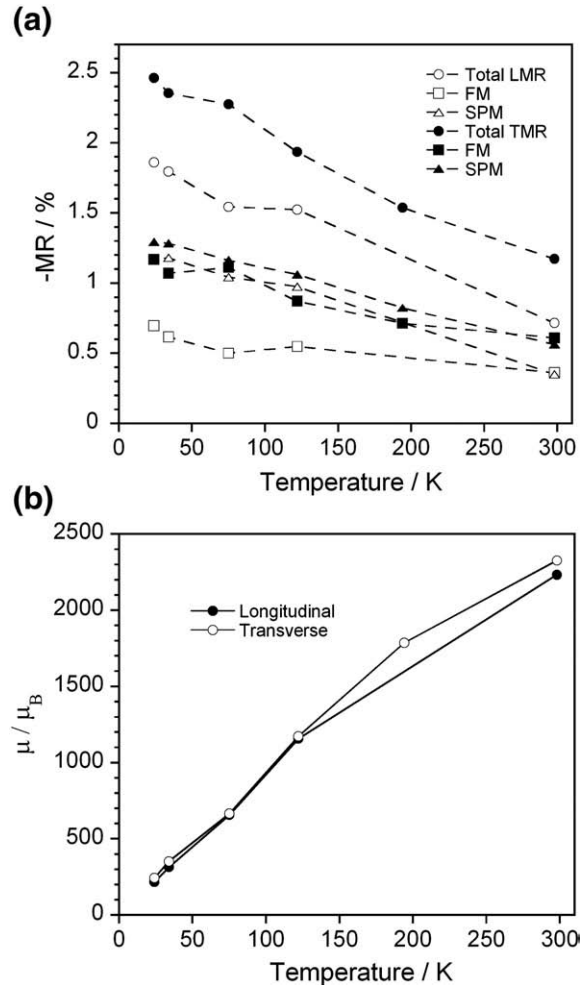


Fig. 12. (a) SPM and FM contributions of the magnetoresistance in both the longitudinal (LMR) and transverse (TMR) geometry as a function of temperature. (b) Dependence of the average magnetic moment (μ) of the SPM regions on the temperature.

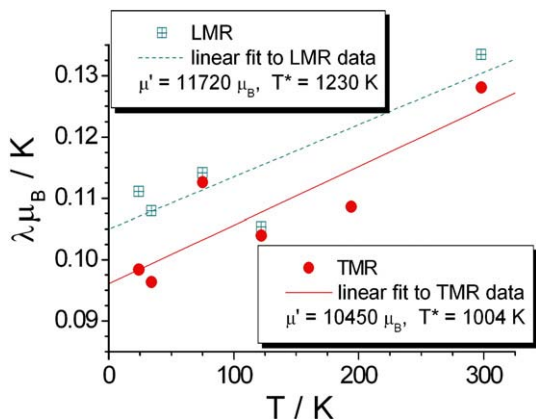


Fig. 13. Parameter $\lambda\mu_B$ as a function of temperature as obtained from magnetoresistance data. The values of μ' and T^* for the longitudinal and transverse magnetoresistance curves are also indicated.

Fig. 13 displays the variation of $\lambda\mu_B$ as a function of temperature for the sample studied. The parameters μ' and T^* are also shown in the figure. Although the data are somewhat scattered, a linear relation with a positive slope over the whole temperature range can be observed. From the interacting SPM model, an average interacting magnetic moment of $\mu' = (11 \pm 1) \times 10^3 \mu_B$ is obtained (where μ_B is the Bohr-magneton). This value is at least five times larger than those obtained with the conventional fitting procedure. The parameter characterizing the strength of the interaction is $T^* = 1120 \pm 120$ K. The T^* values obtained are significantly higher than the maximum temperature of the measurement, which explains why the relative SPM contribution appears to be independent of the temperature of the measurement.

4. Discussion

4.1. Properties of the samples

In order to obtain Co–Ag/Ag multilayer samples with the maximum attainable magnetoresistance ratio, many deposition parameters were optimized by using a pre-defined electrolyte composition. After the optimization of the Co^{2+} concentration and the Co deposition current density, the Ag deposition potential was tuned by applying a method originally developed for the optimization of the electrodeposition of Co–Cu/Cu multilayers. The present work showed that the optimization method is appropriate also for the Co–Ag system and probably for many others in which the more noble and the less noble metals can be codeposited in the so-called normal codeposition mode.

By varying the thickness of both Co and Ag layers, a GMR of about 1% could be achieved for the following nominal layer thicknesses: $d_{\text{Co}} = 3$ nm, $d_{\text{Ag}} = 6$ nm. The increase in any of the layer thicknesses led to a decrease in GMR due to the decrease in interface density, while at smaller Ag layer thickness the loss in GMR could be ascribed to the incomplete separation of the neighbouring Co layers and the partial ferromagnetic coupling of these layers. In this respect, the electrodeposited Co–Ag/Ag multilayers investigated in this study were similar to many other electrodeposited multilayer systems. It is remarkable that the optimum layer thicknesses are usually smaller when the lattice distances of the pure magnetic and non-magnetic metals are closer to each other (like for the Ni–Cu or the Co–Cu pairs).

However, the difference between the lattice parameters of the fcc–Ag and the metastable fcc–Co is rather large. This can be the explanation why neither fcc Co could be detected nor an fcc superlattice with intermediate lattice distances was observed but only hcp Co was found. The dominant orientation of the fcc–Ag and hcp–Co crystals were found to be (111) and (001), respectively, because both crystal planes exhibit a

sixfold symmetry (these are the most densely packed planes) and the atomic distances are quite close to each other. These distances are: $d_{\text{Ag–Ag}} = 0.2887$ nm and $d_{\text{Co–Co}} = 0.2507$ nm; hence, the lattice mismatch is the smallest among the possible crystal plane pairs with identical symmetry. However, since the potentiodynamic curves also showed a hindered Co nucleation on Ag (and probably the nucleation of Ag on Co is similarly hindered), one can conclude that the crystallization of the multilayer constituents took place with some lateral segregation and no superlattice was formed. This assumption is strongly supported by the fact that no satellite peaks were found around any diffraction maximum of the X-ray diffractograms. Indeed, the occurrence of satellite peaks is expected around the main multilayer peak, if there exists any, but in the absence of such peaks the lack of the satellite is a very natural feature of the diffractograms.

The magnetoresistance curves exhibited negative LMR and TMR components and a large saturation field for all multilayer samples. The decomposition of the GMR curves led to a significant SPM fraction in the total GMR, indicating that the individual layers within the multilayer are discontinuous with a characteristic lateral fragmentation distance smaller than the mean free path of the electrons.

The temperature dependence of the GMR showed that the relative SPM contribution is fairly independent of temperature. From an analysis of the results within the framework of the interacting SPM particle model it was found that the data could be fitted in the entire temperature range studied. As predicted by this model, the actual particle size was almost an order of magnitude larger than that obtained with the assumption of a non-interacting SPM behaviour. The high value of the parameter describing the strength of the interaction ($T^* \gg T_{\text{measurement}}$) is a natural explanation for the constant relative SPM contribution throughout the temperature range studied.

It has to be mentioned that the analysis of the SPM contribution as a function of temperature showed that the SPM contribution was independent of the measurement geometry (LMR or TMR), while all difference corresponding to the AMR occurred in the FM contribution. Such data have not been published before because in the study where this method was introduced [30], the LMR component was measured only. The fact that the GMR_{SPM} term does not account for any AMR-type contribution is an indirect evidence for the validity of the model. Namely, if the AMR contribution arises from spin-dependent scattering at the end of electron paths of the type “FM region 1 \rightarrow FM region 1”, then the data have to depend on the measurement geometry and this contribution has to saturate at the field H_s where the FM component of the GMR also saturates. For the FM component of the GMR, the characteristic electron pathway between two spin-dependent scattering events is “FM region 1 \rightarrow NM region \rightarrow FM region 2”.

For the SPM contribution of GMR, one has to assume the following electron pathway: “SPM region \rightarrow NM region \rightarrow FM region” or in the opposite direction. If two consecutive spin-dependent scattering events in the same SPM region can be excluded, the SPM component of the GMR has to saturate at the same magnetic field as the magnetization of the SPM regions. Also, since the magnetization direction of the SPM region is different from that of the FM region, the SPM contribution should be void of any AMR contribution. This is in good agreement with the present finding. It has to be noted as well that the occurrence of electron paths “SPM region 1 \rightarrow NM region \rightarrow SPM region 2” was found to be negligible in ED multilayer systems [14,30,32,33] as opposed to conventional granular metals [34–36], and this was found to be true also for the present samples.

4.2. Comparison with former works on Co/Ag and Co–Ag/Ag multilayers

A common feature of all electrodeposited Co–Ag/Ag multilayers described in former works [9–12] was that saturation of the magnetoresistance could not be achieved up to about 800 kA/m, similarly to the present study. As to the magnitude of the GMR, Ueda

et al. [9–11] have found values of the order of 5% at room temperature whereas in the present work and in the study of Fedosyuk et al. [12], the GMR remained below 1% at the same temperature.

In order to understand this discrepancy, we need to invoke the findings of van Alphen and de Jonge [37] on sputtered Co/Ag multilayers. These authors have established from magnetic and magnetoresistance measurements that in their sputtered Co/Ag multilayers the magnetic Co layer is continuous only if it has a thickness of at least 1 nm. As a consequence, for Co-layers below this thickness, the magnetic layer will consist of fine-sized Co-regions with SPM behaviour, whereas for Co layers thicker than about 1 nm the magnetic layers exhibit an ordinary FM behaviour. For a Co-layer thickness of 2 nm, the room-temperature GMR increased from about 1% to 7% for sputtered Co/Ag multilayers [37] when increasing the Ag layer thickness from 0.5 nm to 4 nm, after which a slight decrease of the GMR with Ag layer thickness was observed. On the other hand, for a Co layer thickness of 0.6 nm, the GMR values rose quickly to around 8% by around 1 nm Ag layer thickness and showed a slight decrease beyond about 3 nm only. The higher GMR values for the Co/Ag multilayers with a 0.6 nm Co layer were attributed to the granular nature of the magnetic layer, i.e., in this case the magnetic layers consist of small SPM entities and electron transition between them contributes to spin-dependent scattering events leading finally to a GMR effect. For a Co layer of 2 nm thickness, the multilayers are of normal FM/NM type, although the authors conclude from the magnetization data that no antiferromagnetic coupling between the FM layers exists. Similarly high GMR values (typically between 5 and 10%) were obtained at room temperature also on Co/Ag multilayers prepared with molecular-beam epitaxy (MBE) with 0.6 nm thick Co layers when the Ag layer thickness was varied between 1 nm and 4 nm [38]; nevertheless, the GMR observed should at least partly arise from a granular type behaviour due to the very thin Co layer, as it can be judged from the high magnetoresistance saturation field. This is also supported by the fact that, for an Ag layer thickness of 2.5 nm, the GMR reduced strongly for thicker Co layers [38]. For Co layer thicknesses around and above 2 nm (i.e., for Co layers with clear FM behaviour) the GMR was already as small as about 1% only [38]. It should be noted furthermore that all the above listed GMR values for multilayers in the Co–Ag system, including the electrodeposited ones both from previous reports [9–12] and from the present study, are well below the corresponding data obtained in the Co–Cu system by any deposition method as also demonstrated by a direct comparison of the GMR at 5 K for sputtered Co/Cu and Co/Ag multilayers [39]. This difference can be attributed to the fact that the lattice mismatch between Co and Ag amounts to about 14% in the fcc phase whereas the lattice mismatch is merely 2% for the fcc–Co and fcc–Cu pairs. This means that the large lattice mismatch introduces a significant interfacial energy during the growth of Co/Ag multilayers and this prevents the formation of a coherent fcc superlattice structure [39]. This fact might also be the reason for the lack of a GMR oscillation in Co/Ag multilayers [37,39] for sufficiently thick FM Co layers.

According to the analysis of the results on our electrodeposited Co–Ag/Ag multilayers, we can conclude that neither the NM Ag layers nor the Co-rich magnetic layers are fully continuous, although there are definitely some regions of the magnetic layers which exhibit FM behaviour. Our room-temperature GMR values are comparable to corresponding results on MBE-grown Co(2–4 nm)/Ag(2.5 nm) multilayers. The shape of the $MR(H)$ curves and the size of the GMR reported by Fedosyuk et al. [13] indicate a very similar behaviour. Nevertheless, the range of film thickness where the highest GMR is observed in the present study does not overlap with the majority of results published by others. The work of Lee et al. [40] was the only one in which the layer thicknesses are similar to those reported here. The difference with that work is the preparation method (*d.c.* sputtering) and hence, as it is expected, the GMR value is also higher. The coincidence is that the highest magnetore-

sistance was detected in sputtered multilayers with thicknesses similar to those reported by the present study.

5. Summary and conclusion

Co–Ag/Ag multilayers were obtained by electrochemical deposition from a perchlorate type bath. The deposition conditions (electrolyte concentration of Co^{2+} , Co deposition current density, Ag deposition potential) and the thicknesses of both types of layers were optimized for maximizing the magnetoresistance ratio. The GMR achieved was about 1% at room temperature and 2.5% at 24 K. The magnetoresistance curves saturated at high magnetic fields only ($H_s > 640$ kA/m). The SPM contribution to the magnetoresistance was high throughout the temperature range studied. The SPM contribution was well elucidated within the framework of the model of interacting SPM regions. It was found that the layers do not form a continuous fcc superlattice due to the large difference in the lattice constants of the pure fcc–Co and fcc–Ag, but the preferred orientation of the crystals (fcc–Ag with (111) and hcp–Co with (001) texture) ensures the identical rotational symmetry and minimizes the lattice mismatch.

Acknowledgements

This work was supported by the Hungarian Scientific Research Fund (OTKA) through grant # K-60821. One of the authors (J. Garcia-Torres) thanks the Departament d'Innovacio, Universitat i Empresa of the Generalitat de Catalunya and the Fons Social Europeu for financial support. The closed-cycle He-cryostat was kindly donated by the Humboldt Foundation, Germany.

References

- [1] M.N. Baibich, J.M. Broto, A. Fert, F. Nguyen Van Dau, F. Petroff, P. Etienne, G. Creuzet, A. Friederich, J. Chazelas, *Phys. Rev. Lett.* 61 (1988) 2472.
- [2] G. Binasch, P. Grünberg, F. Saurenbach, W. Zinn, *Phys. Rev. B* 39 (1989) 4828.
- [3] M. Alper, K. Attenborough, R. Hart, S.J. Lane, D.S. Lashmore, C. Younes, W. Schwarzacher, *Appl. Phys. Lett.* 63 (1993) 2144.
- [4] C.A. Ross, *Ann. Rev. Mater. Sci.* 24 (1994) 159.
- [5] W. Schwarzacher, D.S. Lashmore, *IEEE Trans. Magn.* 32 (1996) 3133.
- [6] I. Bakonyi, L. Péter, in: S. Krongelb, et al., (Eds.), *Magnetic Materials, Processes and Devices VIII. 196th Meeting of The Electrochemical Society, Honolulu, Hawaii, USA, October 17–22, 1999, The Electrochemical Society Proceedings Series, vol. 2004–23, 1999, p. 227.*
- [7] L. Péter, I. Bakonyi, in: G. Staikov (Ed.), *Electrocrystallization in Nanotechnology, Wiley-VCH, Weinheim, Germany, 2007, p. 242.*
- [8] S. Valizadeh, G. Holmbom, P. Leisner, *Surf. Coat. Technol.* 105 (1998) 213.
- [9] H. Zaman, S. Ikeda, Y. Ueda, *IEEE Trans. Magn.* 33 (1997) 3517.
- [10] Y. Ueda, T. Houga, A. Yamada, H. Zaman, *J. Magn. Soc. Japan* 23 (1999) 120.
- [11] C.L.S. Rizal, A. Yamada, Y. Hori, S. Ishida, M. Matsuda, Y. Ueda, *Phys. Status Solidi (C)* 1 (2004) 1756.
- [12] V.M. Fedosyuk, W. Schwarzacher, T.A. Tochitskij, S.A. Sharko, *Metallofiz. Noveishie Tekhnol.* 22 (2000) 17.
- [13] V. Weinhacht, L. Péter, J. Tóth, J. Pádár, Zs Kerner, C.M. Schneider, I. Bakonyi, *J. Electrochem. Soc.* 150 (2003) C507.
- [14] I. Bakonyi, L. Péter, Z. Rolik, K. Kiss-Szabó, Z. Kupay, J. Tóth, L.F. Kiss, J. Pádár, *Phys. Rev. B* 70 (2004) 054427.
- [15] L. Péter, Q.X. Liu, Zs. Kerner, I. Bakonyi, *Electrochim. Acta* 49 (2004) 1513.
- [16] L. Péter, J. Pádár, E. Tóth-Kádár, Á. Cziráki, P. Sóki, L. Pogány, I. Bakonyi, *Electrochim. Acta* 52 (2007) 3813.
- [17] E. Gomez, J. Garcia-Torres, E. Valles, *Anal. Chim. Acta* 602 (2007) 187.
- [18] E. Gomez, J. Garcia-Torres, E. Valles, *J. Electroanal. Chem.* 615 (2008) 213.
- [19] S.K.J. Lenczowski, C. Schönenberger, M.A.M. Gijs, W.J.M. de Jonge, *J. Magn. Magn. Mater.* 148 (1995) 455.
- [20] E. Chassaing, *J. Electrochem. Soc.* 148 (2001) C690.
- [21] I. Bakonyi, E. Tóth Kádár, J. Tóth, L.F. Kiss, L. Pogány, Á. Cziráki, C. Ulhaq-Bouillet, V. Pierron-Bohnes, A. Dinia, B. Arnold, K. Wetzig, *Europhys. Lett.* 58 (2002) 408.
- [22] R.C. O Handley, *Modern Magnetic Materials – Principles and Applications*, Wiley, New York, 2000.
- [23] L. Péter, Á. Cziráki, L. Pogány, Z. Kupay, I. Bakonyi, M. Uhlemann, M. Herrich, B. Arnold, T. Bauer, K. Wetzig, *J. Electrochem. Soc.* 148 (2001) C168.
- [24] E. Pellicer, E. Gómez, E. Vallés, *Surf. Coat. Technol.* 201 (2006) 2351.
- [25] E. Gómez, E. Pellicer, E. Vallés, *J. Electroanal. Chem.* 556 (2003) 137.
- [26] J. Garcia-Torres, E. Gómez, E. Vallés, *J. Appl. Electrochem.* 39 (2009) 233.
- [27] Q.X. Liu, L. Péter, J. Tóth, L.F. Kiss, Á. Cziráki, I. Bakonyi, *J. Magn. Magn. Mater.* 280 (2004) 60.

- [28] G. Nabyouni, W. Schwarzacher, Z. Rolik, I. Bakonyi, J. Magn. Magn. Mater. 253 (2002) 77.
- [29] M. Prutton, *Thin Ferromagnetic Films*, Butterworths, London, 1964.
- [30] L. Péter, Z. Rolik, L.F. Kiss, J. Tóth, V. Weihnacht, C.M. Schneider, I. Bakonyi, Phys. Rev., B 73 (2006) 174401.
- [31] P. Allia, M. Coisson, P. Tiberto, F. Vinai, M. Knobel, M.A. Novak, W.C. Nunes, Phys. Rev. B 64 (2001) 144420.
- [32] L. Péter, V. Weihnacht, J. Tóth, J. Pádár, L. Pogány, C.M. Schneider, I. Bakonyi, J. Magn. Magn. Mater. 312 (2007) 258.
- [33] Q.X. Liu, L. Péter, J. Pádár, I. Bakonyi, J. Electrochem. Soc. 152 (2005) C316.
- [34] N. Wiser, J. Magn. Magn. Mater. 159 (1996) 119.
- [35] A.E. Berkowitz, J.R. Mitchell, M.J. Carey, A.P. Young, S. Zhang, F.E. Spada, F.T. Parker, A. Hutten, G. Thomas, Phys. Rev. Lett. 68 (1992) 3745.
- [36] J.Q. Xiao, J.S. Jiang, C.L. Chien, Phys. Rev. Lett. 68 (1992) 3749.
- [37] E.A.M. van Alphen, W.J.M. de Jonge, Phys. Rev. B 51 (1995) 8182.
- [38] S. Araki, J. Appl. Phys. 73 (1993) 3910.
- [39] R. Loloee, P.A. Schroeder, W.P. Pratt Jr., J. Bass, A. Fert, Physica B 204 (1995) 274.
- [40] S.F. Lee, Q. Yang, P. Holody, R. Loloee, J.H. Hetherington, S. Mahmood, B. Ikegami, K. Vigen, L.L. Henry, P.A. Schroeder, W.P. Pratt, J. Bass, Phys. Rev. B 52 (1995) 15426.

5.3. Summary and outlook

In this chapter, the preparation of Co-Ag/Ag multilayers by electrodeposition was attempted. The optimization processes for both cobalt and silver layers deposition were revealed essential in order to have multilayers with GMR values as high as possible. GMR was dependent on the individual layer thickness: it increased with individual layer thickness up to a maximum and then dropped off for thicker layers. In spite of the optimization processes, magnetoresistance values as low as around 0.5 % were measured at room temperature, values which increased up to 2 % at 20 K. The structural characterization as well as the numerical analysis of the MR(H) curves indicated that the individual layers were not fully continuous. The different crystal structures of cobalt and silver as well as the large atomic size difference (lattice mismatch of 14 %) are very unfavourable factors for growing continuous and defect-free multilayers in this system. The insufficient structural quality is certainly one of the major reasons for the low GMR values measured even in the physically deposited Co/Ag multilayers. However, we still think that some progress could be made in the electrodeposition of Co-Ag/Ag multilayers. The use of the chloride-based electrolyte employed to grow Co-Ag granular films could be a good candidate to perform the electrodeposition of the multilayered films, the main reason being the smooth films prepared from this bath.

